Journal of Materials Chemistry C

PAPER

View Article Online
View Journal | View Issue

Cite this: J. Mater. Chem. C, 2014, 2, 5124

Synthesis and optical nonlinear property of Y-type chromophores based on double-donor structures with excellent electro-optic activity

Yuhui Yang,[ab] Huajun Xu,[ab] Fenggang Liu,[ab] Haoran Wang,[ab] Guowei Deng,[ab] Peng Si,[ab] Heyan Huang,[ab] Shuhui Bo,*[a] Jialei Liu,[a] Ling Qiu,[a] Zhen Zhen[a] and Xinhou Liu*[a]

Received 14th March 2014
Accepted 15th April 2014

DOI: 10.1039/c4tc00508b

www.rsc.org/MaterialsC

New Y-type chromophores **FTC-yh1** and **FTC-yh2** containing bis(*N*,*N*-diethyl)aniline as a novel electron-donor, thiophene as a π-conjugated bridge and tricyanofuran (TCF) as an acceptor have been synthesized and systematically investigated in this paper. Density functional theory (DFT) was used to calculate the HOMO–LUMO energy gaps and first-order hyperpolarizability (β) of these chromophores. These chromophores showed better thermal stability with their decomposition temperatures all above 240 °C. Most importantly, the high molecular hyperpolarizability of these chromophores can be effectively translated into large electro-optic (EO) coefficients (r_{33}) in poled polymers. The doped film-A containing 25 wt% chromophore **FTC-yh1** displayed a value of 149 pm V^{-1} at 1310 nm, and the doped film-B containing **FTC-yh2** showed a value of 143 pm V^{-1} at the concentration of 25 wt%. These values are almost four times higher than the EO activity of usually reported traditional single (*N*,*N*-diethyl)aniline nonlinear optical (NLO) chromophores **FTC**. High r_{33} values indicated that the double donors of the bis(*N*,*N*-diethyl)aniline unit can efficiently improve the electron-donating ability and reduce intermolecular electrostatic interactions, thus enhancing the macroscopic EO activity. These properties, together with the good solubility, suggest the potential use of the new chromophores as advanced material devices.

1. Introduction

Organic electro-optic (EO) materials have attracted considerable attention over the past two decades because of their potential applications in optical communication and optical data processing technologies.[1–4] As an important branch, organic EO polymers have excellent characteristics with large EO coefficients, ultrafast response times, and easy processing,[3,5–8] so they have shown great promise for applications in recent years, such as high speed EO modulators, switches, directional couplers and so on. However, for practical applications, one of the challenges in preparing excellent EO materials is to develop nonlinear optical (NLO) chromophores with large hyperpolarizability (β) and to reduce adverse strong inter-molecular electrostatic interactions among the chromophore molecules.[9,10] Thus, chromophores with large β and weak intermolecular electrostatic interaction, as the decisive factor, must be designed and prepared.

Generally, the NLO chromophores have the structures of a donor–π–acceptor which usually possess a rod-like structure. So the strong intermolecular dipole–dipole interactions will develop in the polymeric system and further make the poling-induced noncentrosymmetric alignment of chromophores a daunting task.[11] Furthermore, accompanying with the increased concentration of chromophore moieties in the materials, these intermolecular dipole–dipole interactions would become stronger, which would finally lead to a decreased EO activity.[12] Thus, how to decrease these interactions, and efficiently translate the large β values of the organic chromophores into a high macroscopic EO activity of polymers, has become one of the major problems in optimizing organic NLO materials.[13–15] To achieve higher EO activity and suppress the dipole interaction among chromophores, rational molecular designs of dipole chromophores have been made from the conjugated push–pull molecules. Many efforts have been carried out to design and synthesize novel NLO chromophores, seeking to engineer NLO molecules both microscopically (β) and macroscopically (r_{33}).[13,16,17] However, it should be noted that the majority of these works were focused on the conjugated bridge and acceptor structures.[18–25] The electron donors, which are important components of NLO chromophores, have received little attention. Among all the materials studied, the dipolar

[a]Key Laboratory of Photochemical Conversion and Optoelectronic Materials, Technical Institute of Physics and Chemistry, Chinese Academy of Sciences, Beijing 100190, PR China. E-mail: boshuhui@mail.ipc.ac.cn; xhliu@mail.ipc.ac.cn; xinhouliu@foxmail.com; Fax: +86-01-62554670; Tel: +86-01-82543528

[b]University of Chinese Academy of Sciences, Beijing 100043, PR China

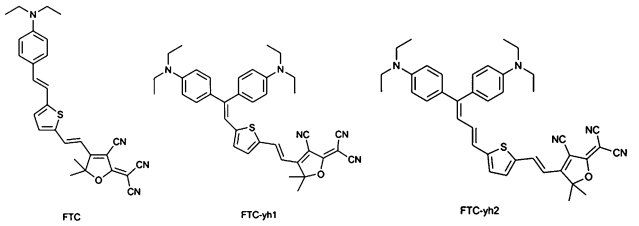

Chart 1 The structure of the chromophore of FTC, FTC-yh1 and FTC-yh2.

chromophores bearing *N*,*N*-dimethyl aniline as a donating group have been widely studied due to their large molecular nonlinearity with significantly enhanced thermo- and photostabilities.[8,20,25–27]

In this paper, we choose the bis(*N*,*N*-diethylaniline) unit as a new donating moiety. Due to its high electron-density and low cost,[28] the bis(*N*,*N*-diethylaniline) unit has been widely studied in the dye-sensitized solar cells (DSCs).[4,28,29] On the one hand, the new donor with two *N*,*N*-diethylaniline units may improve the electron-donating ability and thus may enhance the optical nonlinearity. One of the *N*,*N*-diethylaniline unit can act as both the additional donor and the isolated group (IG). Applying the site isolation principle, the introduction of some IGs into the chromophore moieties is an effective approach to suppress the dipole interactions among chromophores and improve the poling efficiency, thus achieving much larger macroscopic NLO effects.[15,30] On the other hand, as reported, controlling the shape of the chromophore was proven to be an efficient approach for minimizing this interaction and enhancing the poling efficiency.[31] These new chromophores having the double benzene rings with an appropriate angle make the special Y-type structure which is different from the general NLO chromophores showing the rod-like structure. So it may efficiently reduce the intermolecular electrostatic interactions and thus may enhance the macroscopic EO activity. To the best of our knowledge, the novel double donor units rarely appeared in the NLO chromophore before.

Considering the abovementioned advantages, we choose the bis(*N*,*N*-diethylaniline) unit as a new donating moiety. Two new chromophores (in Chart 1) with the bis(*N*,*N*-diethylaniline) unit as a donor were designed and prepared by a facile route from Michler's ketone. They showed great solubility in common organic solvents, good compatibility with polymers, and large EO activity in the poled films. ^{1}H-NMR and ^{13}C-NMR analyses were carried out to demonstrate the preparation of these chromophores. Thermal stability, photophysical properties, DFT calculations and EO activities of these chromophores were systematically studied and were compared with the single-aniline chromophore **FTC** (Chart 1).

2. Results and discussion

2.1. Synthesis and characterization of chromophores

The synthesis of **FTC-yh1**, **FTC-yh2** and traditional **FTC** chromophores is depicted in Schemes 1–3, respectively.

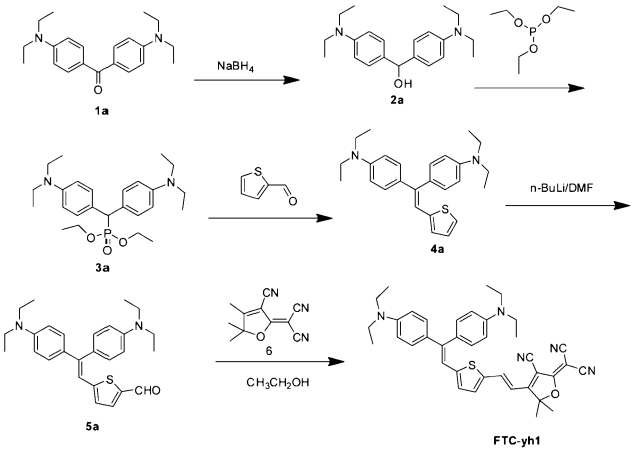

Scheme 1 Chemical structure and synthetic scheme for chromophore FTC-yh1.

Chromophores **FTC-yh1** and **FTC-yh2** were prepared according to different strategies. **FTC-yh1** was obtained in five steps starting from the commercially available Michler's ketone (Scheme 1). Alcohol **2a** was obtained in moderate yield by reduction of the Michler's ketone with sodium borohydride in boiling THF and was then directly converted to phosphonate **3a** using a procedure described in the literature.[32] Phosphonate **3a** was condensed with 2-thenaldehyde by Horner–Emmons reaction in which the proper base plays a key role in determining the yield. We found that replacing the commonly used potassium *tert*-butoxide with sodium hydride produced **4a** with a much improved yield (60%). Treatment of compound **4a** with *n*-BuLi and DMF gave an aldehyde **5a**. The target chromophore **FTC-yh1** was obtained *via* the Wittig reaction of aldehyde **5a** with acceptor TCF in the presence of a catalytic amount of piperidine.

FTC-yh2 was obtained in five steps in a different way (Scheme 2). The crucial reaction involves the creation of an additional double bond and a functional group on the donor of Michlers Ethylketone for later conversion to aldehyde. The reaction of **1b**

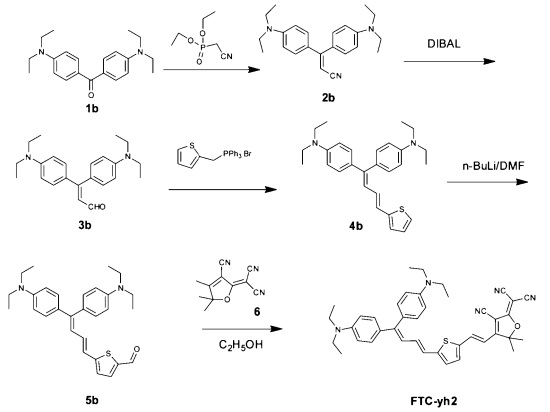

Scheme 2 Chemical structure and synthetic scheme for chromophore FTC-yh2.

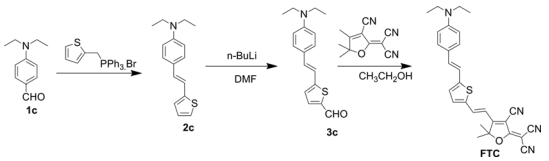

Scheme 3 Chemical structure and synthetic scheme for chromophore FTC.

with diisopropyl (cyanomethyl)-phosphonate using sodium hydride as a base resulted in **2b** with 65% yield. The reduction with DIBAL-H followed by acid hydrolysis converts the nitrile group on **2b** into the corresponding aldehyde **3b** with 83% yield. Aldehyde **3b** was condensed with 2-thienyltriphenylphosphonate bromide by Wittig condensation to gain **4b**. As expected, after introduction of the thiophene bridge by Wittig condensation, treatment of compound **4b** with *n*-BuLi and DMF gave an aldehyde **5b**. The target chromophore **FTC-yh2** was obtained *via* the Knoevenagel condensation reaction of aldehyde **5b** with acceptor TCF in the presence of a catalytic amount of piperidine.

The traditional **FTC** chromophore was obtained in three steps starting from the commercially available aldehyde **1c** (Scheme 3). The aldehyde **1c** was condensed with 2-thienyltriphenylphosphonate bromide by Wittig condensation to gain **2c**. As expected, after introduction of the thiophene bridge by Wittig condensation, treatment of compound **2c** with *n*-BuLi and DMF gave an aldehyde **3c**. The target chromophore **FTC** was obtained *via* the Knoevenagel condensation reaction of aldehyde **3c** with acceptor TCF in the presence of a catalytic amount of piperidine.

All the chromophores were fully characterized by ^{1}H-NMR, ^{13}C-NMR, and mass spectroscopy. These chromophores possess good solubility in common organic solvents, such as dichloromethane, chloromethane and acetone.

2.2. Thermal analysis

NLO chromophores must be thermally stable enough to withstand encountered high temperatures (>200 °C) in electric field poling and subsequent processing of chromophore/polymer materials. Thermal properties of the two chromophores were measured by Thermogravimetric Analysis (TGA). Both **FTC-yh1** and **FTC-yh2** showed excellent stability. The decomposition temperatures (T_d) of chromophores **FTC-yh1** and **FTC-yh2** were 249 °C and 247 °C, respectively, while, the traditional single donor **FTC** showed a T_d of 242 °C. Therefore, the double donor chromophores have a better thermo-stability than the traditional **FTC** chromophore. Therefore, the T_d of the two chromophores was high enough for the application in EO device preparation.

2.3. Optical properties

In order to reveal the effect of double donors on the intramolecular charge transfer (ICT) of dipolar chromophores, UV-Vis absorption spectra of three chromophores ($c = 1 \times 10^{-5}$ mol L^{-1}) were measured in a series of aprotic solvents with different polarity so that the solvatochromic behavior of these chromophores could be investigated to explore the polarity of chromophores in a wide range of dielectric environments (Fig. 1 and 2). The spectrum data are summarized in Table 1. The synthesised chromophores exhibited a similar $\pi \rightarrow \pi^*$ intramolecular charge-transfer (ICT) absorption band in the visible region. **FTC-yh1** and **FTC-yh2** showed the maximum absorption (λ_{max}) of 725 nm and 750 nm in $CHCl_3$ respectively. With extending a double bond into the chromophore **FTC-yh1**, the λ_{max} of **FTC-yh2** chromophore red shifted by 25 nm to 750 nm. These values are exceptionally large compared to the traditional **FTC** (λ_{max} of 676 nm in $CHCl_3$) with single aniline donor and the same π-conjugated bridge and acceptor. The double donors shifted the ICT absorption band of the chromophore to the lower energy. As shown in Fig. 1 and 2, the peak wavelength of **FTC-yh1** and **FTC-yh2** showed a bathochromic shift of 71 nm from dioxane to chloroform, displaying the larger solvatochromism compared with the single donor **FTC** chromophore (55 nm in Table 1). The resulting spectrum data confirmed that the chromophores with double donors were more easily polarizable than the single donor **FTC**. These analyses implied that the double donors of bis(*N*,*N*-diethyl)-aniline improved the electron-donating capability and increased the polarizability of **FTC-yh1** and **FTC-yh2**.

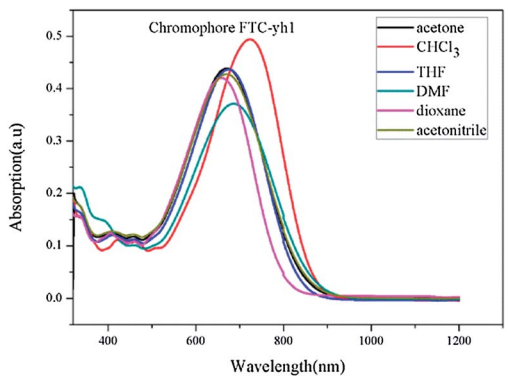

Fig. 1 UV-Vis absorption spectra in different solvents of chromophore **FTC-yh1** ($c = 1 \times 10^{-5}$ mol L^{-1}).

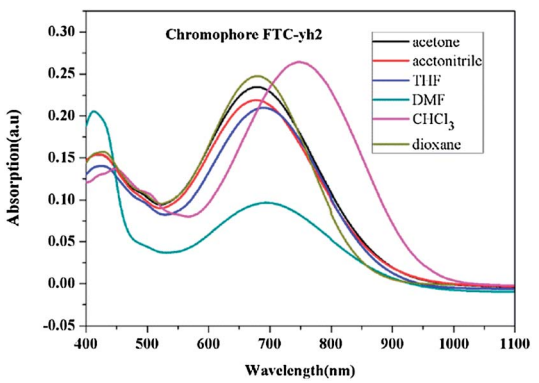

Fig. 2 UV-Vis absorption spectra in different solvents of chromophore **FTC-yh2** ($c = 1 \times 10^{-5}$ mol L^{-1}).

Table 1 Summary of thermal optical properties and EO coefficients of chromophores FTC, FTC-yh1 and FTC-yh2

	T_d[a](°C)	λ_{max}[b](nm)	λ_{max}[c](nm)	$\Delta\lambda$[d] (nm)	r_{33}[e] (pm V^{-1})
FTC	242	676	621	55	39
FTC-yh1	249	725	654	71	149
FTC-yh2	247	750	679	71	143

[a] T_d was determined by an onset point, and measured by TGA under a nitrogen atmosphere at a heating rate of 10 °C min^{-1}. [b] λ_{max} was measured in $CHCl_3$. [c] λ_{max} was measured in dioxane. [d] $\Delta\lambda = \lambda_{max}^{b} - \lambda_{max}^{c}$. [e] r_{33} values were measured at the wavelength of 1310 nm.

As reported,[33] the observed blueshifts (H type) or redshifts (J type) of dyes in optical absorption spectra are due to the interplay of optical selection rules modified through intermolecular interactions. However, we find that there is no dipole–dipole interaction in the solvents at this low concentration of our chromophores (10^{-5} mol L^{-1}). By testing the different concentrations of these three chromophores in $CHCl_3$, we have proved that there was no shift in the shape of the absorption peaks shown in Fig. 3. In our work, the absorption peak shifts in the different solvent were measured for solvatochromism which was related to the polarization and nonlinearity of the chromophores.

2.4. Theoretical calculations

In order to model the ground state molecular geometries, the HOMO–LUMO energy gaps and β values of these chromophores were calculated. The DFT calculations were carried out at the hybrid B3LYP level by employing the split valence 6-31 g (d, p) basis set.[34–36] The data obtained from DFT calculations are summarized in Table 2.

The frontier molecular orbitals are often used to characterize the chemical reactivity and kinetic stability of a molecule and to obtain qualitative information about the optical and electrical properties of molecules.[36–38] Besides, the HOMO–LUMO energy gap is also used to understand the charge transfer interaction occurring in a chromophore molecule.[38–40] In the case of these chromophores, Fig. 4 represents the frontier molecular orbitals of chromophores **FTC**, **FTC-yh1** and **FTC-yh2**. According to Fig. 4, it is clear that the electronic distribution of the HOMO is delocalized over the thiophene linkage and benzene ring, whereas the LUMO is mainly constituted by the acceptor moieties.[38]

The HOMO and LUMO energy were calculated by DFT calculations as shown in Table 2. For double donor chromophores **FTC-yh1** and **FTC-yh2**, the effect of double donor structures narrows the energy gap between the HOMO and LUMO energy with ΔE values of 1.963 eV and 1.766 eV respectively. By contrast, the ΔE value of **FTC** is 2.032 eV. It can be concluded that the LUMO energy of chromophore **FTC** is 0.021 eV larger than that of **FTC-yh1** (−3.192 eV *vs.* −3.123 eV), while the HOMO energy of **FTC** is 0.048 eV smaller than that of **FTC-yh1** (−5.224 eV *vs.* −5.176 eV). The same trend can be observed in chromophore **FTC-yh2**. This may result from the fact that the double donor structure influences the HOMO energy to a greater extent than the LUMO energy. The HOMO–LUMO gaps of **FTC-yh1** (1.963 eV) and **FTC-yh2** (1.766 eV) are lower than **FTC** (2.032 eV), and this indicates that **FTC-yh1** and **FTC-yh2** should exhibit better ICT and NLO property than **FTC**. This is well supported by the facts that the lower is the optical gap, the greater possibility will be the ICT and higher nonlinearity.[38]

The HOMO–LUMO gap was also investigated by cyclic voltammetry (CV). It showed an energy gap (ΔE) value of 1.353 eV for **FTC-yh1** and 1.212 eV for **FTC-yh2**, while the chromophore **FTC** exhibited a ΔE value of 1.529 eV.[8] This comparison demonstrated that the double donors narrowed the energy gap indicating the excellent ICT of the double donor chromophores. This result corresponded with the conclusion of UV-Vis spectra analysis and the DFT results.

Further, the theoretical microscopic β was calculated by Gaussian 03. The β value is related to the substituent, molecular configuration, and intramolecular charge-transfer.[41] As the reference reported earlier, the β has been calculated at the 6-31 g (d, p) level.[42] From this, the scalar quantity of β can be computed from the x, y, and z components according to the following equation:

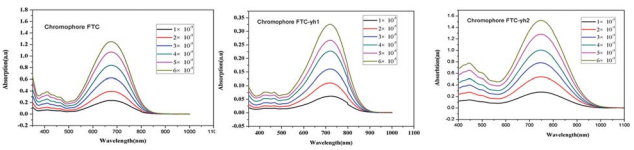

Fig. 3 UV-Vis absorption spectra of different concentrations of three chromophores in $CHCl_3$.

Table 2 Data from DFT calculations[a]

Chromophores	E_{HOMO}/eV	E_{LUMO}/eV	ΔE^b/eV	ΔE^c/eV	β_{max}^{d}/ 10^{-30} esu
FTC	−5.224	−3.192	2.032	1.529.	883
FTC-yh1	−5.176	−3.213	1.963	1.353	713
FTC-yh2	−5.038	−3.272	1.766	1.212	995

[a] $\Delta E = E_{LUMO} - E_{HOMO}$. [b] Results were calculated by DFT. [c] Results were from the cyclic voltammetry experiment. [d] β values were calculated using Gaussian03 at the B3LYP/6-31 g(d) level and the direction of the maximum value is directed along the charge transfer axis of the chromophores.

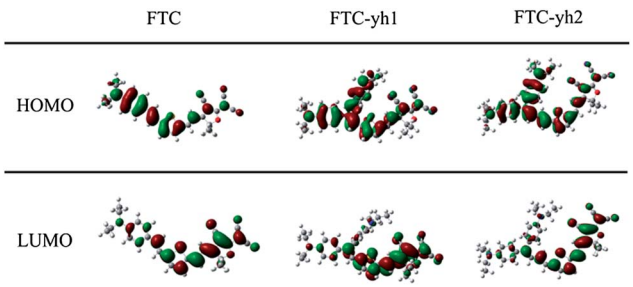

Fig. 4 The frontier molecular orbitals of chromophores FTC, FTC-yh1 and FTC-yh2.

$$\beta = (\beta_x^2 + \beta_y^2 + \beta_z^2)^{1/2} \quad (1)$$

where $\beta_i = \beta_{iii} + \frac{1}{3}\sum_{i \neq j}(\beta_{ijj} + \beta_{jij} + \beta_{jji}), i, j \in (x, y, z)$

Due to the double donors with the stronger electron-donating ability and better conjugated system, chromophore **FTC-yh2** showed a larger β value than the other two chromophores, while chromophore **FTC-yh1** exhibited the smallest β value (713×10^{-30} esu). It may be revealed by the optimized configurations (Fig. 5) that chromophore **FTC-yh1** possessed a less coplanar geometry compared to the **FTC** chromophore, due to the double benzene ring with an angle in **FTC-yh1**. As for **FTC-yh2**, on the one hand, with extending a double bond from **FTC-yh1**, the steric hindrance between the aromatic groups indeed decreases with the lengthening of the ethylenic spacer.[4] On the other hand, **FTC-yh2** has a better conjugation effect which can be verified in the UV-Vis data. Due to the above-mentioned features, **FTC-yh2** with the largest β value is not hard to understand.

Chromophore **FTC-yh1** possessed a little smaller β value, but it showed a larger r_{33} value in the next section. Many factors can affect the r_{33} value. One important factor may be the less electrostatic interaction for **FTC-yh1** between the chromophore molecules. Besides, due to the improved coplanar geometry, the electrostatic interaction between the chromophore molecules was enhanced which led to **FTC-yh2** a little smaller r_{33} than **FTC-yh1**.

As above stated, we have not come to an exact ascertainment that our double donors of Y-type chromophore based bis(*N*,*N*-diethyl)aniline unit are different from the general NLO chromophores. These new chromophores have an obvious advantage in transferring the microscopic β to macroscopic electro-optic effect.

2.5. Electric field poling and EO property measurements

For studying EO property derived from these chromophores, a series of guest–host polymers were generated by formulating the chromophores into amorphous polycarbonate (APC) using dibromomethane as a solvent. The resulting solutions were filtered through a 0.2 μm PTFE filter and spin-coated onto indium tin oxide (ITO) glass substrates. Films of doped polymers were baked in a vacuum oven at 80 °C overnight to ensure the removal of the residual solvent. The corona poling process was carried out at a temperature of 10 °C above the glass transition temperature (T_g) of the polymer. The r_{33} values were measured using the Teng-Man simple reflection technique at the wavelength of 1310 nm using a carefully selected thin ITO electrode with low reflectivity and good transparency in order to minimize the contribution from multiple reflections.[43]

The r_{33} values of films containing chromophores **FTC-yh1** (film-A), **FTC-yh2** (film-B) and **FTC** (film-C) were measured in different loading densities, as shown in Fig. 6. Traditional chromophore **FTC** with the single *N*,*N*-diethylaniline donor gained the r_{33} value from 12 pm V^{-1} (10 wt%) to 39 pm V^{-1} (25 wt%), while the r_{33} values of chromophore **FTC-yh1** were gradually improved from 30 pm V^{-1} (10 wt%) to 149 pm V^{-1} (25 wt%). The similar trend of enhancement was also observed for chromophore **FTC-yh2**, whose r_{33} values increased from 50 pm V^{-1} (10 wt%) to 143 pm V (25 wt%). When the chromophore loading density was up to 25 wt%, the r_{33} value of film B was 143 pm V^{-1}. However, as the loading density increases from 25 wt% to 30 wt%, the film-B displayed a downward trend. To our regret, the film-A with the 30 wt% loading density of **FTC-yh1** presents an obvious phase separation.

Through the outcome above, we can obviously see that the chromophores with the bis(*N*,*N*-diethylaniline) unit as a donor have nearly 4 times higher r_{33} value than the chromophore **FTC**, illustrating that the double donors of the chromophores significantly increase their macroscopic EO activity. This may be explained by the fact that one of the donors could be also acted as the isolation group. As reported earlier,[44] the introduction of some isolation groups into the chromophore moieties to further control the shape of the chromophore could be an efficient approach to minimize interactions between the chromophores. So the double donor chromophores have an obvious advantage in translating β into r_{33} and thus increased the macroscopic EO activity.

As shown in Fig. 6, when the concentration of chromophores in APC is low, film B displayed a larger r_{33} value than film A. As the chromophore loading density increases, this trend is

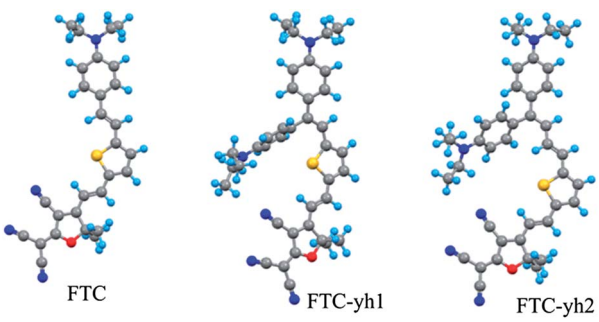

Fig. 5 The optimized structure of chromophores FTC, FTC-yh1 and FTC-yh2.

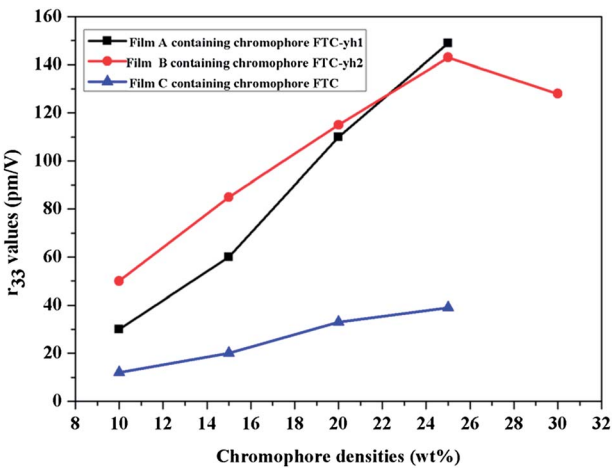

Fig. 6 EO coefficients of NLO thin films as a function of chromophore loading densities.

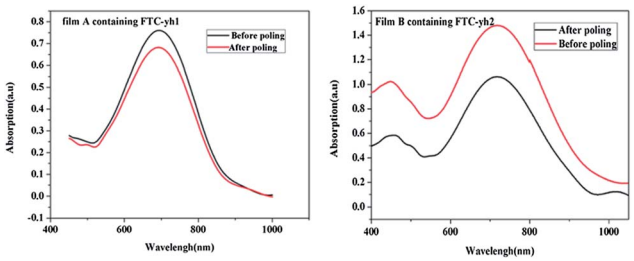

Fig. 7 UV-Vis absorption spectra of E–O polymers before and after poling.

inversed. This can be explained, when, at a low-density range, the intermolecular dipolar interactions are relatively weak. **FTC-yh2** had a larger β and was easily poled which displayed a larger r_{33} value. As the chromophore loading density increases, **FTC-yh2** with a better coplanar geometry presented a stronger negative effect of inter-chromophore dipole–dipole interactions which displayed a smaller r_{33} value.

In order to verify the effect of chromophore structure on the NLO activity, the order parameter (Φ) was calculated by measuring UV-Vis absorption spectra (see Fig. 7). After the corona poling, the dipole chromophores in the polymer were aligned, and the absorption curve decreased due to birefringence. From the absorption changes, the order parameter (Φ) for films can be calculated from the absorption changes according to the following equation: $\Phi = 1 - A_1/A_0$, in which A_1 and A_0 are the respective absorptions of the polymer films after and before corona poling. The order parameter (Φ) of poled films at a loading density of 10 wt% was calculated. The Φ value of film-A (**FTC-yh1**/APC) is 17%, while that of film-B (**FTC-yh2**/APC) is 28% (Fig. 7). The difference in the order parameter indicates that film-B containing chromophore **FTC-yh2** has weaker interchromophore electrostatic interactions and is more easily poled than film-A. At the same time, with an extended double bond into **FTC-yh1**, **FTC-yh2** has an advantage of molecular rotation and thus makes it move more easily under the electric field. This result corresponded with the conclusion of UV-Vis spectra analysis.

3. Experimental

3.1. Materials and instrumentation

^{1}H NMR spectra were recorded by an Advance Bruker 400(400 MHZ) NMR spectrometer (tetramethylsilane as an internal reference). The MS spectra were obtained on MALDI-TOF-(Matrix Assisted Laser Desorption/Ionization Time of Flight) on a BIFLEXIII(Broker Inc.) spectrometer. The UV-Vis spectra were recorded on a Cary 5000 photo spectrometer. The TGA was determined by a TA5000-2950TGA (TA Co) with a heating rate of 10 °C min^{-1} under the protection of nitrogen. Cyclic voltammetry (CV) experiments were performed on a CHI660D electrochemical workstation by a cyclic voltammetry (CV) technique in CH_3CN solution, using two platinum wires as the working and counter electrodes, respectively, and a saturated calomel electrode as the reference electrode in the presence of 1 mM *n*-tetrabutylammoniumperchlorate as the supporting electrolyte. All chemicals, commercially available, are used without further purification unless otherwise stated. The DMF and THF were freshly distilled prior to their use. The 2-dicyanomethylene-3-cyano-4-methyl-2,5-dihydrofuran (TCF) acceptor was prepared according to the literature.[45]

3.2. Synthesis

3.2.1 Synthesis of compound 3a. Alcohol **2a** was obtained in moderate yield by reduction of the Michler's ketone with sodium borohydride in boiling THF and was then directly converted to phosphonate **3a** using a procedure described in the literature.[32]

^{1}H-NMR (400 MHz, acetone-d_6): δ = 7.34 (dd, J_{HH} = 8.5 Hz, J_{HP} = 1.5 Hz, 4H, Ar–H), 6.62 (d, J = 8.6 Hz, 4H, Ar–H), 4.21 (d, J = 25.0 Hz, 1H, CH), 3.75–4.08 (m, 4H, CH_2O), 3.34 (m, 8H, CH_2N), 1.33 (t, J = 7.0 Hz, 6H, 2 Me), 1.20 (t, J = 7.0 Hz, 6H, 2 Me), 1.12 (t, J = 7.0 Hz, 6H, 2 Me).

MALDI-TOF: m/z calcd for $C_{25}H_{38}N_2O_3P$: 446.26 $[M]^+$; found: 446.27.

3.2.2 Synthesis of compound 4a. To a suspension of diethyl bis(4-(dimethylamino)phenyl) methylphosphonate **3a** (1.5 g, 3.36 mmol), and thiophene-2-carbaldehyde (336 mg, 3 mmol) in 20 mL dry THF and NaH (0.14 g, 5.6 mmol) were added and the mixture turned yellow. The mixture was stirred at room temperature for 24 h. Saturated NH_4Cl was added and the resulting mixture was extracted with EtOAc (20 × 3 mL). The combined extracts were washed with water and dried over $MgSO_4$. After filtration and removal of the solvent under vacuum, the crude product was purified by column chromatography to give a yellow liquid (0.73 g, 60%).

^{1}H-NMR (400 MHz, acetone-d_6): δ = 7.18 (d, J = 9.0 Hz, 2H, Ar–H), 7.14 (s, 1H, CH), 7.06 (d, J = 5.0 Hz, 1H, CH), 6.99 (d, J = 8.7 Hz, 2H, Ar–H), 6.93 (d, J = 3.6 Hz, 1H, CH), 6.85 (dd, J = 5.0, 3.6 Hz, 1H, CH), 6.80 (d, J = 8.7 Hz, 2H, Ar–H), 6.64 (d, J = 9.0 Hz, 2H, Ar–H), 3.43 (m, 8H, CH_2N), 1.22 (t, J = 7.0 Hz, 6H, 2 Me), 1.15 (t, J = 7.0 Hz, 6H, 2 Me).

^{13}C-NMR (100 MHz, acetone-d_6): δ = 148.56, 148.09, 143.84, 141.69, 132.06, 129.05, 128.85, 127.97, 127.14, 126.61, 125.46, 117.00, 113.07, 112.13, 44.90, 12.99, 12.94.

MALDI-TOF: m/z calcd for $C_{26}H_{32}N_2S$: 404.23 $[M]^+$; found: 404.22.

3.2.3 Synthesis of compound 5a. To a solution of **4a** (1.0 g, 2.47 mmol) in dry THF (20 mL) was added a 2.4 M solution of *n*-BuLi in hexane (1.5 mL, 3.7 mmol) dropwise at −78 °C under a N_2 atmosphere. After this the mixture was stirred at this temperature for 1 h, and the dry DMF (0.23 mL, 3.0 mmol) was introduced. The resulting solution was stirred for another 1 h at −78 °C and then allowed to warm up to room temperature. The reaction was quenched by water. THF was removed by evaporation. The residue was extracted with CH_2Cl_2 (3 × 30 mL). The organic layer was dried by $MgSO_4$ and concentrated *in vacuo*. The residue was purified by column chromatography on a silica gel (hexane–acetone, v/v, 10/1) to obtain a red solid (0.87 g, 82%).

^{1}H-NMR (400 MHz, acetone-d_6): δ = 9.74 (s, 1H, CHO), 7.67 (d, J = 4.0 Hz, 1H, CH), 7.25–7.22 (overlap, 3H, Ar–H, CH), 7.09

(d, J = 4.0 Hz, 1H, CH), 7.02–6.98 (m, 2H, Ar–H), 6.87–6.81 (m, 2H, Ar–H), 6.67 (m, 2H, Ar–H), 3.44 (m, 8H, CH_2N), 1.22 (t, J = 7.0 Hz, 6H, 2 Me), 1.15 (t, J = 7.0 Hz, 6H, 2 Me).

^{13}C-NMR (100 MHz, acetone-d_6): δ = 183.06, 153.68, 148.94, 147.41, 142.10, 137.35, 131.75, 129.49, 129.01, 115.86, 113.07, 111.76, 44.90, 12.93.

MALDI-TOF: m/z calcd for $C_{27}H_{32}N_2OS$: 432.24 $[M]^+$; found: 432.22.

3.2.4 Synthesis of chromophore FTC-yh1. A mixture of aldehydic bridge **5a** (0.85 g, 1.97 mmol) and acceptor **6** (0.43 g, 2.16 mmol) in ethanol (30 mL) was stirred at 75 °C for 4 h in the presence of a catalytic amount of piperidine. After removal of the solvent, the residue was purified by column chromatography on a silica gel (hexane–ethyl acetate, v/v, 4 : 1). A dark solid was obtained (0.45 g, 37%).

^{1}H-NMR (400 MHz, acetone-d_6): δ = 7.98 (d, J = 15.7 Hz, 1H, CH), 7.54 (d, J = 4.2 Hz, 1H, CH), 7.33–7.26 (overlap, 3H, Ar–H, CH), 7.14 (d, J = 4.2 Hz, 1H, CH), 7.01 (d, J = 8.7 Hz, 2H, Ar–H), 6.88 (d, J = 8.7 Hz, 2H, Ar–H), 6.69 (d, J = 9.0 Hz, 2H, Ar–H), 6.46 (d, J = 15.7 Hz, 1H, CH), 3.55–3.39 (m, 8H, CH_2N), 1.79 (s, 6H, 2 Me), 1.25 (t, J = 7.0 Hz, 6H, 2 Me), 1.17 (t, J = 7.0 Hz, 6H, 2 Me).

^{13}C-NMR (100 MHz, acetone-d_6): δ = 177.45, 174.88, 154.58, 154.55, 149.48, 149.27, 149.23, 148.92, 141.19, 139.71, 137.54, 131.81, 131.06, 130.01, 129.11, 125.35, 116.24, 113.47, 113.25, 112.80, 112.06, 111.84, 111.65, 98.62, 97.03, 45.10, 44.96, 26.39, 12.95.

MALDI-TOF: m/z calcd for $C_{38}H_{39}N_5OS$: 613.29 $[M]^+$; found: 613.22.

HRMS (ESI) (M^+, $C_{38}H_{39}N_5OS$): calcd: 614.29481; found: 614.29509.

3.2.5 Synthesis of compound 2b. A 250 mL three-necked flask was charged with NaH (1.5 g, 62.5 mmol) in dry THF (30 mL) under a N_2 atmosphere. Diisopropyl (cyanomethyl)-phosphonate (8.05 g, 0.050 mol) was introduced into the mixture dropwise by a syringe at 0 °C with an ice bath. After the solution became clear, compound **1b** (8.0 g, 0.025 mol) in THF (20 mL) was added. The mixture was refluxed for 24 h. The resulting solution was poured into 100 mL ice water and was extracted with CH_2Cl_2 (3 × 30 mL). The organic layer was dried ($MgSO_4$) and concentrated *in vacuo*, and the residue was purified by column chromatography on a silica gel (hexane–acetone, v/v, 50/1) to obtain a yellow solid (5.57 g, 65%).

^{1}H-NMR (400 MHz, acetone-d_6): δ = 7.33–7.26 (m, 2H, Ar–H), 7.26–7.17 (m, 2H, Ar–H), 6.78–6.73 (m, 2H, Ar–H), 6.72–6.67 (m, 2H, Ar–H), 5.48 (s, 1H, CH), 3.46 (m, 8H, CH_2N), 1.18 (dt, J = 10.4, 7.0 Hz, 12H, 4 Me).

^{13}C-NMR (100 MHz, acetone-d_6): δ = 163.64, 150.23, 149.81, 132.25, 131.17, 126.73, 124.84, 120.52, 111.76, 111.40, 86.95, 44.93, 44.88, 12.94, 12.88.

MALDI-TOF: m/z calcd for $C_{23}H_{29}N_3$: 347.29 $[M]^+$; found: 347.23.

3.2.6 Synthesis of compound 3b. To a solution of **2b** (3.47 g, 10 mmol) in dry toluene (30 mL) was added a 1 M solution of diisobutylaluminum hydride in hexane (20 mL, 20 mmol) by a syringe at −78 °C with a dry ice/acetone bath. The reaction mixture was stirred at −78 °C for 2 h. After the mixture was warmed to room temperature, NH_4Cl solution was added to quench the reaction. The mixture was stirred for 1 h to complete the hydrolysis. The organic solvent was collected and removed *in vacuo*. The residue was purified by column chromatography on a silica gel (hexane–acetone, v/v, 10/1) to yield a red solid (2.9 g, 83%).

^{1}H-NMR (400 MHz, $CDCl_3$): δ = 9.47 (d, J = 8.2 Hz, 1H, CHO), 7.31 (d, J = 8.8 Hz, 2H, Ar–H), 7.19 (d, J = 8.7 Hz, 2H, Ar–H), 6.65 (d, J = 8.7 Hz, 2H, Ar–H), 6.62 (d, J = 8.8 Hz, 2H, Ar–H), 6.39 (d, J = 8.2 Hz, 1H, CH), 3.40 (dd, J = 13.5, 6.6 Hz, 8H, CH_2N), 1.20 (dt, J = 8.9, 6.7 Hz, 12H, 4 Me).

^{13}C-NMR (100 MHz, $CDCl_3$): δ = 194.86, 164.90, 150.42, 149.76, 134.04, 132.05, 127.59, 124.79, 123.11, 111.72, 111.40, 45.36, 45.29, 13.52.

MALDI-TOF: m/z calcd for $C_{23}H_{30}N_2O$: 350.24 $[M]^+$; found: 350.24.

3.2.7 Synthesis of compound 4b. Under a N_2 atmosphere, a mixture of **3b** (2.0 g, 5.7 mmol) and 2-thienyl triphenylphosphonate bromide (3.01 g, 6.86 mmol) in dry THF (20 mL) at room temperature, and NaH (0.82 g, 34.2 mmol) was added. The mixture turned yellow and was stirred at room temperature for 24 h. Saturated NH_4Cl was added and the resulting mixture was extracted with EtOAc (20 × 3 mL). The combined extracts were washed with water and dried over $MgSO_4$. After filtration and removal of the solvent under vacuum, the crude product was purified by column chromatography on a silica gel (hexane–acetone, v/v, 50/1) to obtain a yellow solid (1.47 g, 60%).

^{1}H-NMR (400 MHz, $CDCl_3$): δ = 7.27 (d, J = 8.8 Hz, 2H, Ar–H), 7.21 (d, J = 10.6 Hz, 1H, CH), 7.14 (d, J = 8.7 Hz, 2H, Ar–H), 7.05 (d, J = 3.9 Hz, 1H, CH), 7.02–6.98 (m, 1H, CH), 6.94–6.83 (m, 1H, CH), 6.68–6.60 (m, overlap, 5H, Ar–H, CH), 6.42–6.28 (m, 1H, CH), 3.41–3.34 (m, 8H, CH_2N), 1.22–1.14 (m, 12H, 4Me).

^{13}C-NMR (100 MHz, acetone-d_6): δ = 147.77, 147.53, 147.05, 146.94, 131.88, 131.78, 129.79, 129.00, 128.83, 127.67, 127.05, 126.88, 126.32, 125.39, 124.92, 123.50, 123.23, 122.44, 119.58, 119.01, 111.31, 111.28, 111.09, 110.96, 78.56, 44.10, 44.07, 13.30, 12.21.

MALDI-TOF: m/z calcd for $C_{28}H_{34}N_2S$: 430.24 $[M]^+$; found: 430.07.

3.2.8 Synthesis of compound 5b. In a similar manner as described above, **5b** was synthesized from **4b** as a red solid (82%).

^{1}H-NMR (400 MHz, $CDCl_3$): δ = 9.75 (1H, s, CHO), 7.56 (1H, d, J = 4.0 Hz, CH), 7.23 (2H, d, J = 8.8 Hz, Ar–H), 7.12 (2H, d, J = 8.7 Hz, Ar–H), 7.08 (1H, d, J = 11.5 Hz, CH), 6.94 (1H, d, J = 4.0 Hz, CH), 6.72–6.66 (3H, overlap, Ar–H, CH), 6.63–6.57 (3H, overlap, Ar–H, CH), 3.39 (8H, m, CH_2N), 1.20 (12H, m, 4 Me).

^{13}C-NMR (100 MHz, $CDCl_3$): δ = 206.35, 147.38, 147.10, 146.48, 141.73, 132.07, 131.97, 129.51, 129.01, 127.45, 127.01, 126.85, 124.82, 119.58, 119.41, 111.00, 110.78, 44.32, 12.70.

MALDI-TOF: m/z calcd for $C_{29}H_{34}N_2OS$: 458.24 $[M]^+$; found: 458.28.

3.2.9 Synthesis of chromophore FTC-yh2. In a similar manner as described above, **FTC-yh2** was synthesized from **5b** as a dark solid (38%).

^{1}H-NMR (400 MHz, acetone-d_6): δ = 8.12 (d, J = 15.8 Hz, 1H, CH), 7.64 (d, J = 4.0 Hz, 1H, CH), 7.22 (d, J = 8.9 Hz, 2H, Ar–H), 7.11–7.13 (overlap, 3H, Ar–H, CH), 7.07 (d, J = 11.0 Hz, 1H, CH),

6.92 (d, $J = 15.8$ Hz, 1H, CH), 6.84–6.77 (overlap, 3H, Ar–H, CH), 6.73 (d, $J = 11.0$ Hz, 1H, CH), 6.68 (d, $J = 8.9$ Hz, 2H, Ar–H), 3.40 (m, 8H, CH_2N), 1.86 (s, 6H, 2 Me), 1.20 (m, 12H, 4 Me).

^{13}C-NMR (100 MHz, acetone-d_6): $\delta = 177.48, 175.02, 154.32, 149.81, 148.99, 148.77, 140.47, 139.05, 138.83, 134.96, 133.00, 132.86, 130.53, 130.26, 129.93, 128.49, 126.87, 123.03, 122.83, 113.37, 113.15, 112.67, 112.00, 111.82, 98.98, 97.61, 45.02, 44.79, 26.21, 12.88.$

MALDI-TOF: m/z calcd for $C_{40}H_{41}N_5OS$: 639.30 $[M]^+$; found: 639.26.

HRMS (ESI) (M^+, $C_{40}H_{41}N_5OS$): calcd: 640.31046; found: 640.30990.

3.2.10 Synthesis of compound 2c. In a similar manner as described above, **2c** was synthesized from **1c** as a yellow solid (68%).

^{1}H-NMR (400 MHz, $CDCl_3$): $\delta = 7.33$ (d, $J = 8.9$ Hz, 2H, Ar–H), 7.11–7.07 (m, 1H, CH), 7.01 (d, $J = 16.1$ Hz, 1H, CH), 6.96 (d, $J = 3.4$ Hz, 1H, CH), 6.85 (d, $J = 16.1$ Hz, 1H, CH), 6.64 (d, $J = 8.9$ Hz, 2H, Ar–H), 6.47 (d, $J = 3.4$ Hz, 1H, CH), 3.41–3.31 (m, 4H, CH_2N), 1.17 (t, $J = 7.1$ Hz, 6H, 2 Me).

^{13}C-NMR (100 MHz, $CDCl_3$): $\delta = 148.10, 144.72, 130.66, 129.48, 128.22, 127.95, 127.03, 125.05, 124.67, 123.34, 117.69, 112.45, 112.06, 44.88, 13.21.$

3.2.11 Synthesis of compound 3c. In a similar manner as described above, **3c** was synthesized from **2c** as a red solid (86%).

^{1}H-NMR (400 MHz, $CDCl_3$): $\delta = 9.84$ (s, 1H, CHO), 7.66 (d, $J = 3.9$ Hz, 1H, CH), 7.40 (d, $J = 8.6$ Hz, 2H, Ar–H), 7.12 (d, $J = 15.9$ Hz, 1H, CH), 7.07 (d, $J = 3.9$ Hz, 1H, CH), 7.00 (d, $J = 15.9$ Hz, 1H, CH), 6.68 (d, $J = 8.6$ Hz, 2H, Ar–H), 3.43 (m, 4H, CH_2N), 1.22 (t, $J = 7.0$ Hz, 6H, 2 Me).

^{13}C NMR (101 MHz, $CDCl_3$): $\delta = 181.12, 153.45, 147.45, 139.24, 136.25, 132.73, 129.24, 127.63, 123.73, 122.21, 114.71, 110.74, 43.46, 11.64.$

3.2.12 Synthesis of chromophore FTC. In a similar manner as described above, chromophore **FTC** was synthesized from **3c** as a dark solid (41%).

^{1}H-NMR (400 MHz, $CDCl_3$): $\delta = 7.77$ (d, $J = 15.7$ Hz, 1H, CH), 7.38 (d, $J = 8.6$ Hz, 2H, Ar–H), 7.37 (d, $J = 3.9$ Hz, 1H, CH), 7.09 (d, $J = 15.7$ Hz, 1H, CH), 7.01 (d, $J = 3.9$ Hz, 1H, CH), 6.68 (d, $J = 8.6$ Hz, 2H, Ar–H), 6.57 (d, $J = 15.2$ Hz, 1H, CH), 3.52–3.29 (m, 4H), 1.73 (s, 6H), 1.28–1.14 (m, 6H).

^{13}C-NMR (100 MHz, $CDCl_3$): $\delta = 182.03, 172.86, 153.58\delta$ 148.02, 142.13, 140.08, 139.33, 137.39, 129.07, 111.61, 110.91, 110.21, 108.85, 104.96, 99.53, 96.90, 44.81, 44.55, 24.42, 12.58.

MALDI-TOF: m/z calcd for $C_{28}H_{28}N_4OS$: 468.20 $[M]^+$; found: 468.33.

Conclusions

In this research, two NLO chromophores based on bis(*N*,*N*-diethylaniline) donors have been synthesized and systematically investigated. These chromophores with double donors present Y-type structures and exhibit good thermal stability and large molecular hyperpolarizabilities, which can be effectively translated into very large EO coefficients in poled polymers. The doped film-A containing chromophore **FTC-yh1** displayed a maximum r_{33} value of 149 pm V^{-1} at the doping concentration of 25 wt%, while film-B containing chromophore **FTC-yh2** showed a maximum r_{33} value of 143 pm V^{-1} at 25 wt%. Those consequences indicate that these chromophores with double *N*,*N*-diethylaniline donors could efficiently reduce the inter-chromophore electrostatic interactions and enhance the macroscopic optical nonlinearity. This novel donor chromophore showed promising applications in NLO chromophore synthesis. We believe that these novel Y-type chromophores can be used in exploring high-performance organic EO and photorefractive materials where both thermal stability and optical nonlinearity are of equal importance.

Acknowledgements

We are grateful to the National Nature Science Foundation of China (no. 61101054) for financial support.

Notes and references

1 P. A. Sullivan and L. R. Dalton, *Acc. Chem. Res.*, 2010, **43**, 10–18.
2 L. R. Dalton, P. A. Sullivan and D. H. Bale, *Chem. Rev.*, 2010, **110**, 25–55.
3 Y. Q. Shi, C. Zhang, H. Zhang, J. H. Bechtel, L. R. Dalton, B. H. Robinson and W. H. Steier, *Science*, 2000, **288**, 119–122.
4 F. Dumur, C. R. Mayer, E. Dumas, F. Miomandre, M. Frigoli and F. Secheresse, *Org. Lett.*, 2008, **10**, 321–324.
5 A. M. Costero, M. Parra, S. Gil, R. Gotor, R. Martínez-Mañez, F. Sancenón and S. Royo, *Eur. J. Org. Chem.*, 2012, **2012**, 4937–4946.
6 C. S. T. Verbiest, *Macromol. Rapid Commun.*, 2000, **21**, 1–15.
7 Y. V. Pereverzev, K. N. Gunnerson, O. V. Prezhdo, P. A. Sullivan, Y. Liao, B. C. Olbricht, A. J. P. Akelaitis, A. K. Y. Jen and L. R. Dalton, *J. Phys. Chem. C*, 2008, **112**, 4355–4363.
8 P. A. Sullivan, A. J. P. Akelaitis, S. K. Lee, G. McGrew, S. K. Lee, D. H. Choi and L. R. Dalton, *Chem. Mater.*, 2006, **18**, 344–351.
9 M. Q. He, T. M. Leslie, J. A. Sinicropi, S. M. Garner and L. D. Reed, *Chem. Mater.*, 2002, **14**, 4669–4675.
10 L. Dalton and S. Benight, *Polymers*, 2011, **3**, 1325–1351.
11 L. R. Dalton, A. W. Harper and B. H. Robinson, *Proc. Natl. Acad. Sci. U. S. A.*, 1997, **94**, 4842–4847.
12 A. W. Harper, S. Sun, L. R. Dalton, S. M. Garner, A. Chen, S. Kalluri, W. H. Steier and B. H. Robinson, *J. Opt. Soc. Am. B*, 1998, **15**, 329–337.
13 J. Wu, J. Liu, T. Zhou, S. Bo, L. Qiu, Z. Zhen and X. Liu, *RSC Adv.*, 2012, **2**, 1416.
14 L. R. Dalton, D. Lao, B. C. Olbricht, S. Benight, D. H. Bale, J. A. Davies, T. Ewy, S. R. Hammond and P. A. Sullivan, *Opt. Mater.*, 2010, **32**, 658–668.
15 Z. Li, Q. Q. Li and J. G. Qin, *Polym. Chem.*, 2011, **2**, 2723–2740.
16 C. Zhang, L. R. Dalton, M. C. Oh, H. Zhang and W. H. Steier, *Chem. Mater.*, 2001, **13**, 3043–3050.

17 Y. J. Cheng, J. D. Luo, S. Hau, D. H. Bale, T. D. Kim, Z. W. Shi, D. B. Lao, N. M. Tucker, Y. Q. Tian, L. R. Dalton, P. J. Reid and A. K. Y. Jen, *Chem. Mater.*, 2007, **19**, 1154–1163.
18 R. Andreu, M. A. Cerdan, S. Franco, J. Garin, A. B. Marco, J. Orduna, D. Palomas, B. Villacampa, R. Alicante and M. Allain, *Org. Lett.*, 2008, **10**, 4963–4966.
19 Y. Liao, B. E. Eichinger, K. A. Firestone, M. Haller, J. D. Luo, W. Kaminsky, J. B. Benedict, P. J. Reid, A. K. Y. Jen, L. R. Dalton and B. H. Robinson, *J. Am. Chem. Soc.*, 2005, **127**, 2758–2766.
20 P. Si, J. Liu, Z. Zhen, X. Liu, G. Lakshminarayana and I. V. Kityk, *Tetrahedron Lett.*, 2012, **53**, 3393–3396.
21 D. Briers, L. De Cremer, G. Koeckelberghs, S. Foerier, T. Verbiest and C. Samyn, *Macromol. Rapid Commun.*, 2007, **28**, 942–947.
22 S. R. Hammond, O. Clot, K. A. Firestone, D. H. Bale, D. Lao, M. Haller, G. D. Phelan, B. Carlson, A. K. Y. Jen, P. J. Reid and L. R. Dalton, *Chem. Mater.*, 2008, **20**, 3425–3434.
23 J. D. Luo, M. Haller, H. Ma, S. Liu, T. D. Kim, Y. Q. Tian, B. Q. Chen, S. H. Jang, L. R. Dalton and A. K. Y. Jen, *J. Phys. Chem. B*, 2004, **108**, 8523–8530.
24 S. Liu, M. A. Haller, H. Ma, L. R. Dalton, S. H. Jang and A. K. Y. Jen, *Adv. Mater.*, 2003, **15**, 603–607.
25 A. Leclercq, E. Zojer, S. H. Jang, S. Barlow, V. Geskin, A. K. Y. Jen, S. R. Marder and J. L. Bredas, *J. Chem. Phys.*, 2006, **124**, 044301.
26 R. U. Dominique Roberto, *Organometallics*, 2000, **19**, 1775–1788.
27 P. G. Lacroix, *Chem. Mater.*, 2001, **13**, 3495–3506.
28 K. Tang, M. Liang, Y. Liu, Z. Sun and S. Xue, *Chin. J. Chem.*, 2011, **29**, 89–96.
29 T. Kitamura, M. Ikeda, K. Shigaki, T. Inoue, N. A. Anderson, X. Ai, T. Q. Lian and S. Yanagida, *Chem. Mater.*, 2004, **16**, 1806–1812.
30 W. B. Wu, Q. Huang, G. F. Qiu, C. Ye, J. G. Qin and Z. Li, *J. Mater. Chem.*, 2012, **22**, 18486–18495.
31 W. B. Wu, C. Wang, R. L. Tang, Y. J. Fu, C. Ye, J. G. Qin and Z. Li, *J. Mater. Chem. C*, 2013, **1**, 717–728.
32 S. Zheng, S. Barlow, T. C. Parker and S. R. Marder, *Tetrahedron Lett.*, 2003, **44**, 7989–7992.
33 V. I. Gavrilenko and M. A. Noginov, *J. Chem. Phys.*, 2006, **124**, 044301.
34 R. M. Dickson and A. D. Becke, *J. Chem. Phys.*, 1993, **99**, 3898–3905.
35 M. Frisch, G. Trucks, H. Schlegel, G. Scuseria, M. Robb, J. Cheeseman, J. Montgomery Jr, T. Vreven, K. Kudin and J. Burant, *Gaussian Inc.*, Pittsburgh, PA, 2003.
36 C. Lee and R. G. Parr, *Phys. Rev. A*, 1990, **42**, 193–200.
37 X. Ma, F. Ma, Z. Zhao, N. Song and J. Zhang, *J. Mater. Chem.*, 2010, **20**, 2369.
38 R. V. Solomon, P. Veerapandian, S. A. Vedha and P. Venuvanalingam, *J. Phys. Chem. A*, 2012, **116**, 4667–4677.
39 R. M. El-Shishtawy, F. Borbone, Z. M. Al-Amshany, A. Tuzi, A. Barsella, A. M. Asiri and A. Roviello, *Dyes Pigm.*, 2013, **96**, 45–51.
40 J. Y. Wu, J. L. Liu, T. T. Zhou, S. H. Bo, L. Qiu, Z. Zhen and X. H. Liu, *RSC Adv.*, 2012, **2**, 1416–1423.
41 H. Xu, M. Zhang, A. Zhang, G. Deng, P. Si, H. Huang, C. Peng, M. Fu, J. Liu, L. Qiu, Z. Zhen, S. Bo and X. Liu, *Dyes Pigm.*, 2014, **102**, 142–149.
42 K. S. Thanthiriwatte and K. M. N. de Silva, *J. Mol. Struct.: THEOCHEM*, 2002, **617**, 169–175.
43 C. C. Teng and H. T. Man, *Appl. Phys. Lett.*, 1990, **56**, 1734.
44 W. B. Wu, J. G. Qin and Z. Li, *Polymer*, 2013, **54**, 4351–4382.
45 T. M. L. Mingqian He and J. A. Sinicropi, *Chem. Mater.*, 2002, **14**, 2393–2400.

